LAWRENCE
LIVERMORE
NATIONAL
LABORATORY

LLNL-CONF-404246

ANALYSIS OF DAMAGE TO WASTE PACKAGES CAUSED BY SEISMIC EVENTS DURING POST-CLOSURE

Steven W. Alves, Stephen C. Blair, Steven R. Carlson, Michael Gerhard, Thomas A. Buscheck

May 29, 2008

2008 International High-Level Radioactive Waste Management
Las Vegas, NV, United States
September 7, 2008 through September 11, 2008

Disclaimer

ANALYSIS OF DAMAGE TO WASTE PACKAGES CAUSED BY SEISMIC EVENTS DURING POST-CLOSURE

Steven W. Alves, Stephen C. Blair, Steven R. Carlson, Michael Gerhard, and Thomas A. Buscheck
Lawrence Livermore National Laboratory, P.O. Box 808, Livermore CA, 94551, email: buscheck1@llnl.gov

Abstract — *This paper presents methodology and results of an analysis of damage due to seismic ground motion for waste packages emplaced in a nuclear waste repository at Yucca Mountain, Nevada. A series of three-dimensional rigid body kinematic simulations of waste packages, pallets, and drip shields subjected to seismic ground motions was performed. The simulations included strings of several waste packages and were used to characterize the number, location, and velocity of impacts that occur during seismic ground motion. Impacts were categorized as either waste package-to-waste package (WP-WP) or waste package-to-pallet (WP-P). In addition, a series of simulations was performed for WP-WP and WP-P impacts using a detailed representation of a single waste package. The detailed simulations were used to determine the amount of damage from individual impacts, and to form a damage catalog, indexed according to the type, angle, location and force/velocity of the impact. Finally, the results from the two analyses were combined to estimate the total damage to a waste package that may occur during an episode of seismic ground motion. This study addressed two waste package types, four levels of peak ground velocity (PGV), and 17 ground motions at each PGV. Selected aspects of waste package degradation, such as effective wall thickness and condition of the internals, were also considered. As expected, increasing the PGV level of the vibratory ground motion increases the damage to the waste packages. Results show that most of the damage is caused by WP-P impacts. TAD-bearing waste packages with intact internals are highly resistant to damage, even at a PGV of 4.07 m/s, which is the highest level analyzed.*

I. INTRODUCTION

The concept of drift emplacement of waste packages at Yucca Mountain is illustrated in Figure 1. Waste packages are to be emplaced in horizontal drifts, aligned parallel to the drift axis. Waste packages will be closely spaced (end to end), and waste packages of different sizes may be placed adjacent to each other. During seismic shaking, end-to-end impacts between waste packages (WP-WP impacts), impacts between waste packages and pallets (WP-P impacts), and impacts between waste packages and drip shields may damage the waste packages. Moreover, during the postclosure period, significant changes in the drift environment are expected to occur. These include changes in temperature, relative humidity, and seepage rates; degradation of the drift ground control system and the Engineered Barrier System (EBS) components; and rockfall from the host rock surrounding the drift. Note that the analysis of the environmental changes is addressed elsewhere [1, 2, 3] and is beyond the scope of this paper.

Vibratory ground motion from a remote earthquake may affect several of the primary EBS components. These components include: (a) waste package; (b) waste package internals, which are defined to include all components and materials contained inside the Alloy 22 outer corrosion barrier (OCB); (c) invert, which is composed of a steel framework filled with engineered ballast composed of crushed tuff; (d) emplacement pallet, which rests on the invert, supports the waste package, and is constructed of Alloy 22 end piers and 316 Stainless Steel connector tubes; and (e) the drip shield, which is a structure constructed of Titanium Grade 7 plates and Titanium Grade 29 framework that protects the waste package from seepage water and rockfall.

The waste form packaging design for commercial spent nuclear fuel calls for the spent fuel to be placed in a standardized transportation, aging, and disposable (TAD) canister system, which will be used for packaging pressurized water reactor and boiling water reactor waste forms at the reactor sites. Prior to emplacement in Yucca Mountain, each TAD canister will be inserted into a waste package, consisting of an outer corrosion barrier and a structural inner vessel. The TAD canister and waste package are referred to as the TAD-bearing waste package (or NL/TAD in Fig. 1, because the dimensions are based on the naval-long waste package). The weight, length, and center of gravity for the TAD-bearing waste package are incorporated into the seismic damage models. Also included are calculations for 5-DHLW/DOE SNF codisposal (CDSP) waste packages, containing vitrified defense high-level radioactive waste and U.S. Department of Energy spent nuclear fuel assemblies.

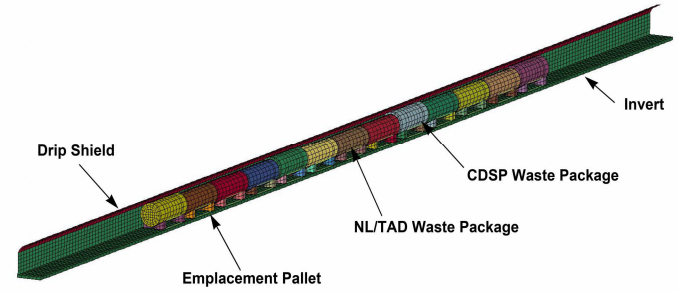

Fig. 1. String of thirteen (nine TAD-bearing and four CDSP) waste packages used in rigid-body simulations. One side of the drip shield has been removed for clarity.

The major EBS components are free-standing structures. The drip shield and the emplacement pallet rest on top of the invert, while the waste package rests on

top of the emplacement pallet. Because the EBS components are unconstrained, impacts can occur between waste packages, drip shields, emplacement pallets, invert, and drift walls in response to significant ground motions. The invert, waste package internals, and waste-form mass are also considered in structural response simulations presented in this paper, as was done in Reference 4.

These components are important because their failure has the potential to directly influence the release of radionuclides or to form diffusive or advective transport pathways to the host rock. The effectiveness of these barriers is potentially compromised by the direct effects of an earthquake, which include vibratory ground motion, fault displacement, and rockfall. The effectiveness of these barriers is also potentially compromised by indirect effects after an earthquake, including in-drift changes in seepage, temperature, and relative humidity.

II. METHODOLOGY

Model calculations are performed with the LS-DYNA finite element code [5]. A typical emplacement drift, 600 m in length, will contain ~100 waste packages of various types. It is desirable to reduce the analysis complexity and run time by representing the mechanical response of the emplacement drift using the minimum number of waste packages necessary without sacrificing the validity of the analysis. Kinematic calculations consider a "string" of multiple waste packages in a section of an emplacement drift. The string is composed of a combination of TAD-bearing waste packages and CDSP waste packages. The mix and number of waste packages is chosen to be representative of the waste package inventory in the repository. The string must have enough waste packages to enable the response of the central waste packages to be independent of the free boundaries at either end of the string.

The following discussion concerns the determination of damaged area on the OCB. For the purpose of this paper, damaged area implies the presence of stress corrosion cracking (SCC) in the OCB, which is a potential pathway for diffusive radionuclide release.

For computational efficiency, the kinematic calculations use relatively coarse finite-element representations of the waste package and pallet as elastic bodies that preserve the mass and dimensions of the components. The kinematic calculations are too coarse to determine the structural deformation or damage from multiple impacts directly. Instead, damage induced by these impacts is calculated from the kinematic impact parameters for WP-WP impacts and for WP-P impacts by using lookup tables calculated from detailed impact analyses. A direct correlation is made between damaged surface area and impact velocity/force, angle of impact, and impact location, allowing the kinematic calculations to represent the damage to multiple waste packages without the penalty of running very detailed finite-element models. The final damaged area from multiple impacts is determined by summing the damaged areas from individual impacts, based on the lookup table and impact parameters. These final damaged areas form the basis of the seismic damage abstractions for Total System Performance Assessment (TSPA).

The kinematic calculations represent an emplacement drift that has partially or completely collapsed, so that the drip shield is pinned in place and moves synchronously with the free field. The report *Drift Degradation Analysis* [3] shows that complete collapse of emplacement drifts in lithophysal rock occurs at a PGV of ~2 m/s or greater and that substantial rock blocks are dislodged at this PGV level in the nonlithophysal rock as well. Even relatively small amounts of rockfall tend to prevent axial separation of drip shield segments. Therefore, the drip shield is represented as a boundary that moves synchronously with the free field for the kinematic calculations.

The input data for the kinematic calculations include the following:

- Seventeen ground motion time histories (Figure 2) for each of the 0.4, 1.05, 2.44, and 4.07 m/s PGV levels. The same kinematic model is used at all PGV levels.
- Friction coefficient for metal-to-metal (WP, pallet, and drip shield) contacts.
- Friction coefficient for metal-to-crushed tuff (invert) contact.
- Elastic material properties of the waste package and pallet.
- Dimensions and masses of the drip shield, waste packages and pallets.

The uncertainty in the ground motions and in the friction coefficients is propagated into the kinematic calculations by Latin Hypercube sampling. Each friction coefficient is independently sampled from a uniform distribution ranging from 0.2 to 0.8. The ground motion number is sampled from a discrete, uniform distribution from 1 to 17. This sampling provides a list of input data in which a given ground motion time series is randomly paired with metal-to-metal and metal-to-invert friction coefficients for each waste package and pallet.

The kinematic calculations were designed to represent the rigid body motions of multiple waste packages, not the structural deformation of each waste package. Each waste package is therefore represented as an elastic body with Young's modulus and Poisson's ratio defined at room temperature. While elastic properties vary with temperature, the use of room-temperature values is a reasonable approximation for the rigid body interactions of the waste packages.

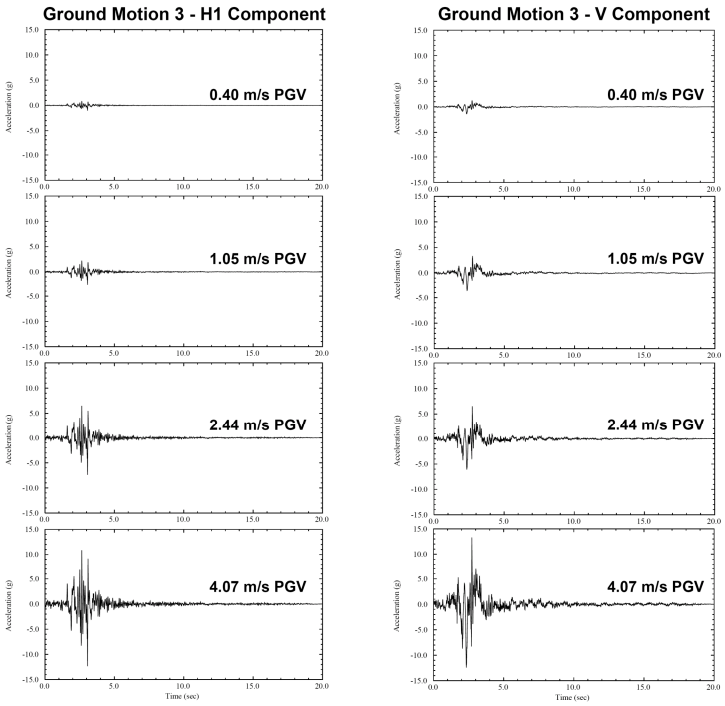

Fig. 2. Typical acceleration time histories at four peak ground velocity (PGV) levels used as input to the kinematic calculations. The H1 direction is parallel to the string of emplaced waste packages.

III. RESULTS

The output data from the kinematic calculations are a set of impact parameters, including:

- Time of impact.
- Relative velocity of the impacting bodies.
- Force between the impacting bodies.
- Relative angle of impact of the impacting bodies.
- Impact location.

For every impact between adjacent waste packages or between a waste package and an emplacement pallet, the time, relative velocity/force, relative angle, and location of the collision were recorded. The corresponding damage from multiple impacts during a given ground motion was determined from a series of lookup tables that relate the relevant impact parameters to the surface area that has exceeded a residual tensile stress criterion. Multiple impacts at the same location were tracked so that excessive damage could not be accumulated at a single location.

Lookup tables for WP-WP impacts were generated from detailed finite-element calculations (Figure 3) for the horizontal impact of a moving waste package onto an initially stationary (but not fixed) waste package. Impact configurations for the TAD-bearing to TAD-bearing WP-WP impact and for the TAD-bearing to CDSP WP-WP impact cases are shown in Figures 4 and 5.

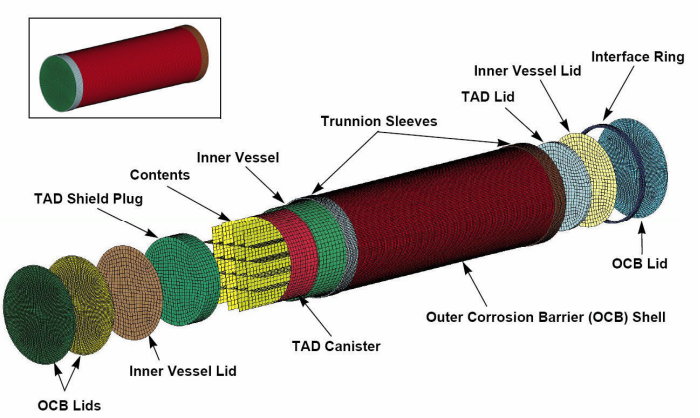

Fig. 3. Detailed representation of the TAD-bearing waste package with intact internals used for waste package damage lookup table analyses.

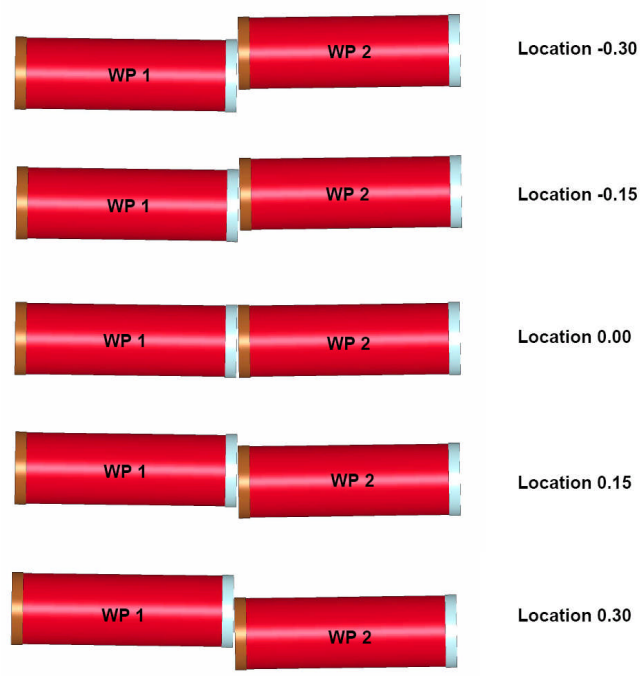

Fig. 4. Impact configurations for TAD-bearing waste package-to-TAD-bearing waste package analyses.

Lookup tables for WP-P impacts were generated from detailed finite-element analyses of side-on impacts of a waste package on an emplacement pallet (Figure 6). The potential for rupture was also assessed, in part, from lookup tables, based on the ultimate tensile strain of Alloy 22 and a "knockdown" factor that accounts for the potential effects of a biaxial stress field and strain rate on the ultimate strain of a material. The knockdown factor provides an initial basis for screening cases with the potential for rupture. If a case exceeded the knockdown factor, the detailed stress state and the occurrence of multiple large impacts were considered to determine whether rupture occurs.

Fig. 5. Impact configurations for CDSP waste package-to-TAD-bearing waste package analyses.

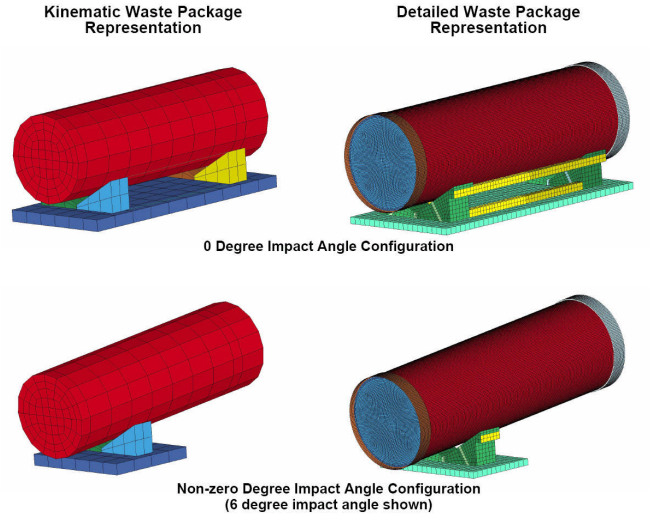

Fig. 6. Kinematic WP-P impact analyses corresponding to the detailed WP-P damage lookup table analyses.

Input data for the lookup table calculations include the temperature for material properties and the residual stress threshold for initiation of stress corrosion cracking (SCC) in deformed areas. Elastic and plastic material properties were set to constant values at 60°C based on data from handbooks or manufacturer's catalogs. This temperature provides bounding values for material properties over a long time scale for the seismic scenario class after 10,000 years. A sensitivity study [4] showed that the damaged area is relatively insensitive to elevated temperatures during the first 10,000 years.

The residual stress threshold for initiation of SCC on the OCB is defined as a range from 90 to 105% of the yield strength of Alloy 22. Uncertainty associated with this range is propagated into TSPA by defining abstractions that are a function of the residual stress threshold and by interpolating between the damaged areas at the 90, 100, and 105% residual stress thresholds to capture this uncertainty in TSPA.

Multiple lookup tables are defined to represent a range of future states of TAD-bearing or CDSP waste packages. The potential for general corrosion reducing the OCB thickness is addressed by reducing the OCB thickness from its initial value of 25.4 mm. For WP-WP impacts, the future states are: 23-mm-thick OCB with intact internals, 23-mm-thick OCB with degraded internals, and 17-mm-thick OCB with degraded internals. These thicknesses are the spatially averaged thickness of the OCB, because average thickness is anticipated to be the key parameter for structural response.

The rationale for the three future states is as follows. The first state, 23-mm-thick OCB with intact internals, approximates relatively early waste package behavior with 2.4 mm of corrosion, beneath an intact drip shield. The third state, 17-mm-thick OCB with degraded internals, approximates late waste package behavior with 8.4 mm of corrosion, beneath an intact drip shield. The second state, 23-mm-thick OCB with degraded internals, approximates a period between the other two states. For the states with degraded internals, credit is not taken for the stainless steel inner vessel, for the TAD canister, or for the fuel baskets as structural elements. This approach maximizes calculated structural deformation and damaged area if the stainless steel elements do not degrade quickly in a dilute chemical environment. Each WP-WP lookup table has multiple entries for impact velocity, impact angle, and impact location.

The lookup tables for WP-P impacts are structured in a manner similar to those for WP-WP impacts. The future states are 23-mm-thick OCB with intact internals, 23-mm-thick OCB with degraded internals, and 17-mm-thick OCB with degraded internals. Each WP-P lookup table has multiple entries for impact force, impact angle, and impact location.

Damaged area and rupture condition are determined for the OCB of the waste package. The OCB shell and outer OCB lids are considered to comprise the OCB for this purpose. All of these components are Alloy 22. The damaged area is computed by determining the area of the OCB surface that has a residual maximum (first) principal stress that exceeds one of three damage levels (90, 100, and 105% of yield strength). The residual stresses are obtained by allowing the impact event to complete and then applying damping to the analysis for 0.05 seconds. The yield strength for Alloy 22 at 60°C is 352 MPa, so

the three stress levels correspond to 316 MPa, 352 MPa, and 369 MPa, respectively. An element of the finite element mesh contributes to the damaged area if any of the outer, inner, or middle surfaces has a residual stress that exceeds the damage level. The area for an element is only counted once if multiple surfaces of that element exceed the damage level.

The determination of damaged area is performed using LS-PREPOST, which is a postprocessor for LS-DYNA [5]. The area fraction of a part that exceeds a residual maximum principal stress level is determined using the "volume of material failure" option in LS-PREPOST. Since the OCB is modeled with shell elements, the "volume of material failure" option produces an area of material failure. The failure levels for maximum principal stress are set at 90, 100, and 105% of the yield strength of Alloy 22, and the area is determined by taking the area fractions that exceed the levels at the end of the analysis and multiplying by the surface area of the part, as shown in Figure 7. A typical fringe plot of the damaged area is shown in Figure 8. The damaged areas are determined separately for the OCB shell and lids. For WP-WP impacts, the damaged areas on the OCB shell and lids for a waste package are summed to obtain a damaged area for that waste package. The damaged areas are determined separately for both of the impacting waste packages. For WP-P impacts, the damaged areas for the OCB shells and both of the OCB lids are recorded separately for postprocessing.

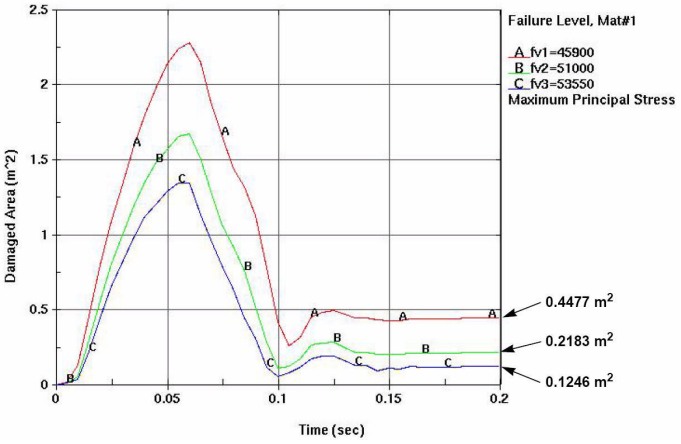

Fig. 7. Typical curves used for computing damaged area of the OCB shell at 90% (red), 100% (green), and 105% (blue) of yield strength.

The rupture condition of a waste package is determined by comparing the maximum effective strain from all elements on the outer and inner surfaces of the OCB to the ultimate tensile strain limit. Determination of the strain limit is discussed in Reference 4. For uniaxial tension, the maximum effective strain limit is 0.57. For biaxial tension, the maximum effective strain limit can be as low as 0.285, based on a triaxiality factor of 2.0.

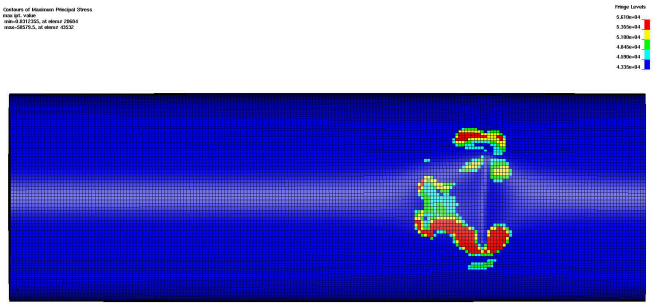

Fig. 8. A typical fringe plot showing the damaged area on the OCB shell. Dark blue area corresponds to < 90% of yield strength; while light blue to green corresponds to > 90%; yellow corresponds to > 100%; and red corresponds to > 105% of yield strength, respectively.

The OCB rupture condition for a single impact is determined using LS-PREPOST to perform a multi-layer screening process as illustrated in Figure 9. The maximum effective strain on the OCB (on both the outer and inner surfaces) is used to identify potential rupture. Figure 10 shows a typical maximum effective strain history for the outer surface of the OCB. If the maximum effective strain does not exceed 0.285 at any time during the analysis, rupture is screened out. If the maximum effective strain for any elements of the OCB exceeds 0.285 at any time, then the triaxiality factor is computed for the stress state of those elements on the appropriate surface. The elements that have effective strain exceeding 0.285 at some time during the analysis are determined visually (Figure 11). The OCB shell and lids are considered simultaneously for both WP-WP impacts and WP-P impacts to obtain the rupture condition for a waste package.

On the basis of the approach described above, no single impact was determined to cause rupture of the OCB. However, an approach was developed to account for the effects of multiple impacts in order to assess the rupture condition of the waste packages. The deformation of the OCB shell was observed from single impact calculations of a waste package and a pallet in order to estimate the probability of rupture if multiple impacts were to occur. Only WP-P impacts were considered because the deformation was much larger than for WP-WP impacts.

This approach identifies two states of the rupture condition for a waste package: incipient rupture and rupture. Incipient rupture is defined as a state in which a waste package has been subjected to one impact during a seismic event that causes deformation such that another large impact during a later seismic event will cause rupture of the waste package. A waste package is in a state of incipient rupture at the end of a kinematic seismic analysis if one and only one impact causing deformation associated with this state occurs during that analysis. If

two or more such impacts occur for a waste package during a kinematic seismic analysis, then the waste package is in a state of rupture.

For waste packages with intact internals, the calculated probabilities of rupture and incipient rupture are zero. The presence of the intact inner vessel and TAD canister (in the case of the TAD-bearing waste package) limits the deformation. For waste packages with degraded internals, non-zero probabilities of rupture and incipient rupture are calculated for the higher PGV levels.

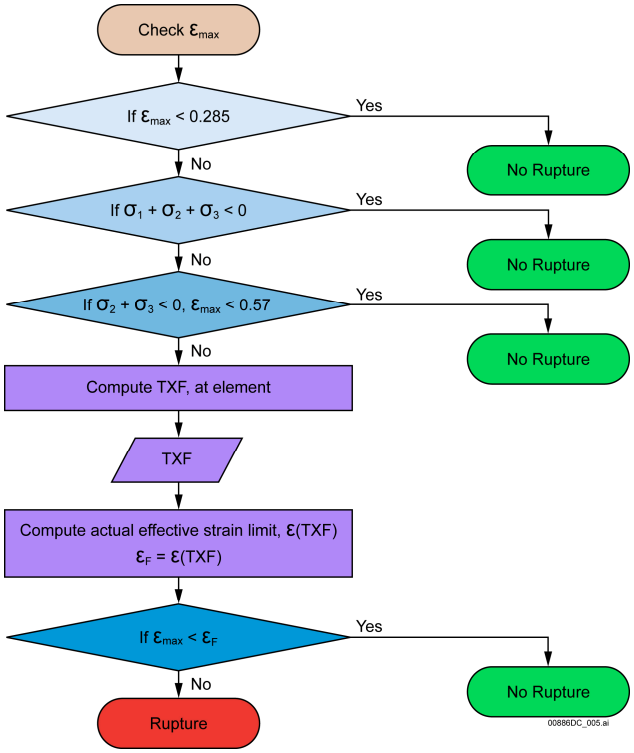

Fig. 9. Flow chart showing the decision process for screening rupture for a specific element, based on stress-strain state.

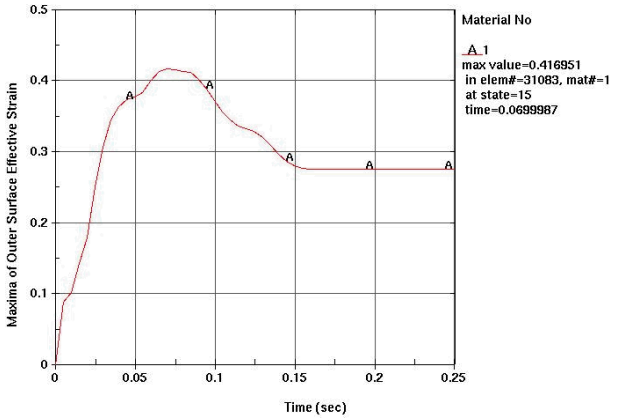

Fig. 10. A typical maximum effective strain history for the outer surface of the OCB shell.

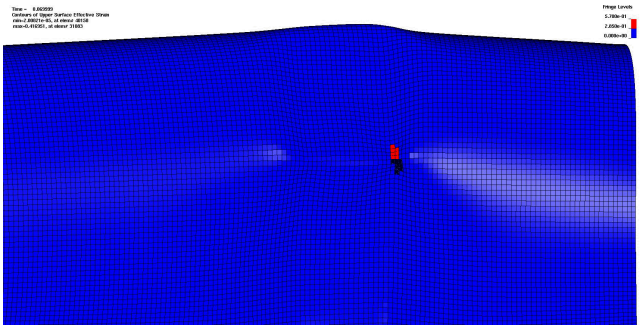

Fig. 11. A typical fringe plot showing the area (red) of the OCB shell with an effective strain > 0.285.

IV. VALIDATION

In order to validate the multiple step approach (coarse kinematic analyses and detailed impact analyses) used for computing damaged area on a waste package OCB, detailed waste package models were subjected to earthquake ground motion at low PGV. An example of a model is shown in Figure 12. These analyses were performed for the waste package with a 17-mm-thick OCB and degraded internals.

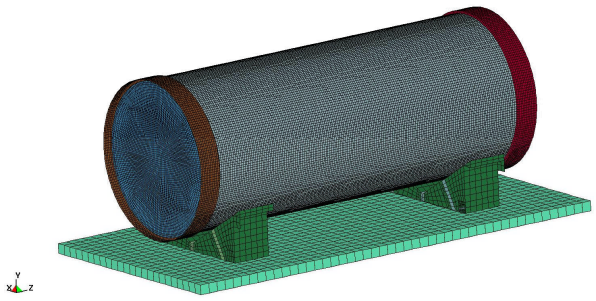

Fig. 12. Single detailed CDSP waste package model subjected to seismic ground motion.

The realizations were chosen by observing which kinematic analyses included the maximum damaged areas, but did not involve interaction with the drip shield or neighboring waste packages. Waste packages in a single realization were modeled by modifying the friction parameters as in the kinematic analyses. The simulation interval was chosen to include only the interval in which damaging impacts for the corresponding waste package had occurred in the kinematic analyses. At the end of this time, the ground motion was stopped, and the waste package stresses were allowed to relax for 0.5 seconds.

For both the TAD-bearing and CDSP waste packages, the detailed analyses show that the kinematic analyses over-predict the damaged area for the low PGV ground motions considered. For the TAD-bearing waste package, the detailed analyses predicted essentially negligible damaged areas. For the CDSP waste package, the detailed analyses predicted damaged areas smaller than the corresponding kinematic analyses, with several

of the detailed analyses predicting essentially negligible damaged areas. Figure 13 shows an example of the damaged area computed from the detailed analyses.

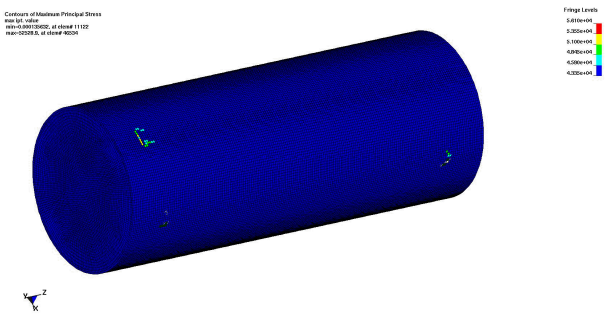

Fig. 13. Typical fringe plot showing the damaged area on the OCB shell for a single detailed waste package subjected to ground motion. The dark blue area corresponds to < 90% of yield strength; light blue to green corresponds to > 90%; yellow corresponds to > 100%; and red corresponds to > 105% of yield strength.

These analyses show that, while the kinematic approach to modeling waste packages subjected to seismic excitation does not yield damaged area estimates that match more detailed simulations, the kinematic approach does overestimate the potential for damage at low PGV levels. Thus, the relatively efficient kinematic approach is a reasonable alternative to performing numerous detailed analyses that are extremely computation-intensive with multiple waste packages for multiple realizations and ground motion levels.

V. CONCLUSIONS

The following conclusions can be drawn from the results presented in this paper and in Reference 4.

1. Increasing the PGV level of the vibratory ground motion increases the damage to the waste packages.
2. Most of the damage to waste packages from vibratory ground motion is caused by waste package-to-pallet rather than waste package-to-waste package impacts.
3. Uncertainty and variability of material properties due to temperature have an insignificant influence on damage to the waste packages due to vibratory ground motion.
4. The TAD-bearing waste package with minor corrosion of the outer corrosion barrier and intact internals is highly resistant to damage, even at PGV levels of 4.07 m/s.
5. Rupture associated with vibratory ground motion is predicted for only a small number of waste packages and only occurs at the higher levels of PGV, and only with degraded internals.
6. Detailed single waste package models subjected to seismic ground motion show that the kinematic/detailed-impact analysis approach overestimates damaged areas for low PGV levels.

ACKNOWLEDGMENTS

This work was performed under the auspices of the U.S. Department of Energy by Lawrence Livermore National Laboratory under Contract DE-AC52-07NA27344, and was supported by the Yucca Mountain Project Lead Laboratory, Sandia National Laboratories. Sandia is a multiprogram laboratory operated by Sandia Corporation, a Lockheed Martin Company, for the United States Department of Energy's National Nuclear Security Administration under contract DE-AC04-94AL85000. The United States Government retains and the publisher, by accepting the article for publication, acknowledges that the United States Government retains a non-exclusive, paid-up, irrevocable, world-wide license to publish or reproduce the published form of this manuscript, or allow others to do so, for United States Government purposes. The statements expressed in this article are those of the authors and do not necessarily reflect the views or policies of the United States Department of Energy, Sandia National Laboratories, or Lawrence Livermore National Laboratory.

REFERENCES

1. SNL, *Multiscale Thermohydrologic Model,* ANL-EBS-MD-000049, Rev 03, AD 01, Sandia National Laboratories, Las Vegas, Nevada (2007).
2. BSC (Bechtel SAIC Company), *Drift-Scale Coupled Processes (DST and TH Seepage) Models.* MDL-NBS-HS-000015, REV 02, Bechtel SAIC Company, Las Vegas, Nevada (2005).
3. BSC (Bechtel SAIC Company), *Drift Degradation Analysis.* ANL-EBS-MD-000027 REV 03, Bechtel SAIC Company, Las Vegas, Nevada (2004).
4. SNL, *Mechanical Assessment of Degraded Waste Packages and Drip Shields Subjected to Vibratory Ground Motion,* MDL-WIS-AC-000001, REV 00, Sandia National Laboratories, Las Vegas, Nevada (2007).
5. Livermore Software Technology Corporation, *LS-DYNA Keyword User's Manual.* Version 970. Livermore, CA (2003).